Published Ahead of Print on August 14, 2020 as 10.1212/WNL.0000000000010498

OPEN

Neurology®
The most widely read and highly cited peer-reviewed neurology journal
The Official Journal of the American Academy of Neurology

AMERICAN ACADEMY OF NEUROLOGY®

Neurology Publish Ahead of Print
DOI: 10.1212/WNL.0000000000010498

Association of specific biotypes in patients with Parkinson disease and disease progression

Linbo Wang, PhD[#], Wei Cheng, PhD[#], Edmund Rolls, DPhil, DSc, Fuli Dai, MSc, Weikang Gong, PhD, Jingnan Du, MSc, Wei Zhang, BSc, Shouyan Wang, PhD, Fengtao Liu, MD, Jian Wang, MD, Peter Brown, MD and Jianfeng Feng, PhD

The Article Processing Charge was funded by the Shanghai Municipal Science and Technology Major Project and ZJLab.

Author Affiliations:

From the Institute of Science and Technology for Brain-inspired Intelligence (L.W., C.W., E.R., F.D, W.K., J. D., W.Z., S.W., J.F.), Fudan University, Shanghai, 200433, PR China;

Key Laboratory of Computational Neuroscience and Brain-Inspired Intelligence (L.W., C.W., J. D., W.Z., S.W., J.F.) (Fudan University), Ministry of Education, Shanghai, 200433, PR China;

Department of Computer Science (E.R., J.F.), University of Warwick, Coventry CV4 7AL, United Kingdom;

Oxford Centre for Computational Neuroscience (E.R.), Oxford, United Kingdom;

Department of Neurology & National Clinical Research Center for Aging and Medicine (F.L., J.W.), Huashan Hospital, Fudan University, 12 Wulumuqi Zhong Road, Shanghai 200040, China;

Medical Research Council Brain Network Dynamics Unit at the University of Oxford (P.B.), Mansfield Road, Oxford OX1 3TH, United Kingdom;

Nuffield Department of Clinical Neurosciences (P.B.), University of Oxford, Level 6, West Wing, John Radcliffe Hospital, Oxford OX3 9DU, United Kingdom.

#These authors contributed equally to the work.

Corresponding author: Professor Jianfeng Feng, Email: jffeng@fudan.edu.cn; jianfeng64@gmail.com

Figures: 5

Tables: 2

Supplemental files (Dryad: doi.org/10.5061/dryad.xsj3tx9bf): 4 tables, 13 figures

Study Funding

This study is sponsored by The Michael J. Fox Foundation for Parkinson's Research. J.Feng is supported by the 111 Project (NO.B18015), the key project of Shanghai Science & Technology (No.16JC1420402), National Key R&D Program of China (No 2018YFC1312900), National Natural Science Foundation of China (NSFC 91630314), Shanghai Municipal Science and Technology Major Project (No.2018SHZDZX01) and

ZJLab. W.Cheng is supported by grants from the National Natural Sciences Foundation of China (No.81701773, 11771010), Sponsored by Shanghai Sailing Program (No. 17YF1426200). W.Cheng is also sponsored by Natural Science Foundation of Shanghai (No. 18ZR1404400). J.Zhang is supported by grants from the National Natural Science Foundation of China (No. 61573107), and also sponsored by Natural Science Foundation of Shanghai (No. 17ZR1444200). Jian Wang is sponsored by Ministry of Science and Technology of China [grant number: 2016YFC1306500, 2016YFC1306504] and National Nature Science Foundation of China [grant number: 81771372]. Fengtao Liu is sponsored by National Nature Science Foundation of China [grant number: 81701250].

Disclosure

The authors report no disclosures relevant to the manuscript.

Abstract

Objective

To identify biotypes in newly diagnosed Parkinson's disease patients and test whether these biotypes could explain inter-individual differences in longitudinal progression.

Methods

In this longitudinal analysis, we use a data-driven approach clustering PD patients from the Parkinson's Progression Markers Initiative (PPMI) (n = 314, age = 61.0 ± 9.5, 34.1% female, 5 years follow-up). Voxel-level neuroanatomical features were estimated using deformation-based morphometry (DBM) of T1-weighted MRI. Voxels whose deformation values were significantly correlated ($P < 0.01$) with clinical scores (MDS-UPDRS-Parts I-III, MDS-UPDRS-total, tremor score, and postural instability and gait difficulty score) at baseline were selected. Then, these neuroanatomical features were subjected to hierarchical cluster analysis. Changes in the longitudinal progression and neuroanatomical pattern were compared between different biotypes.

Results

Two neuroanatomical biotypes were identified: (i) biotype 1 (n = 114) with subcortical brain volumes smaller than heathy controls; (ii) biotype 2 (n = 200) with subcortical brain volumes larger than heathy controls. Biotype 1 had more severe motor impairment, autonomic dysfunction, and very much worse REM sleep behavior disorder than biotype 2 at baseline. Although disease duration at initial visit and follow-up were similar between biotypes, PD patients with smaller subcortical brain volume had poorer prognosis, with more rapid decline in several clinical domains and in dopamine functional neuroimaging over an average of five years.

Conclusion

Robust neuroanatomical biotypes exist in PD with distinct clinical and neuroanatomical pattern. These biotypes can be detected at diagnosis, and predict the course of longitudinal progression, which should benefit trial design and evaluation.

Glossary

ADL = activities of daily living; ESS = Epworth Sleepiness Scale; GDS = Geriatric Depression Scale; HVLT = Hopkins Verbal Learning Test; MDS-UPDRS = Movement Disorder Society–sponsored revision of the Unified Parkinson's Disease Rating Scale; MoCA = Montreal Cognitive Assessment; QUIP = Questionnaire for Impulsive-Compulsive Disorders in Parkinson's Disease; RBD = REM sleep behavior disorder; RBDSQ = REM Sleep Behavior Disorder Screening Questionnaire; SCOPA-AUT = Scales for Outcomes in Parkinson's Disease–Autonomic; STAI = State-Trait Anxiety Inventory; UPSIT = University of Pennsylvania Smell Identification Test.

Introduction

Parkinson's disease (PD) patients present heterogeneous motor and non-motor clinical manifestations and have a variable prognosis.[1, 2] Although the diagnosis of PD is dependent on the presence of tremor, bradykinesia and rigidity, some non-motor phenomena — for example, rapid eye movement (REM) sleep behaviour disorder (RBD), hyposmia and depression— can precede motor deficits by several years. Conversely, as the disease progresses, non-motor problems such as autonomic disturbances, sleep disorders and cognitive impairment can dominate the clinical picture in some patients.[1] Recent evidence suggests that PD may have several biotypes,[3-9] but their identity and neurobiological basis remains poorly understood.[2] Assuming that homogeneous groups of patients are more likely to share pathological features, recognition of different subcategories of PD patients may be key to better understanding underlying biological mechanisms, predicting disease profile and progression, and eventually designing more efficient personalized clinical trials.[2, 3]

Subtypes of PD have previously been defined mainly according to clinical symptoms and demographic characteristics.[3-8] However, cluster results are only as good as the data that underpins them, and the depths of phenotypic information used by these studies were variable, resulting in quite heterogeneous and controversial clusters.[2] In addition, these clinical data-driven PD subtype classification systems may suffer from lack reproducibility.[10] An alternative to subtyping PD patients on the basis of co-occurring clinical symptoms is to identify neuroanatomical biotypes, by clustering subjects according to shared neuroanatomical signatures, which can objectively capture different aspects of patient characteristics. Studying brain neuroanatomical patterns of PD provides an opportunity to examine biological heterogeneity in vivo.[11] Data-driven methods provide an unbiased approach to detect groups of patients with similar profiles across multiple neuroanatomical feature dimensions, and so may yield a more refined description of heterogeneity in PD. T1-weighted MRI is an especially suitable modality to describe brain anatomy with high resolution, and quantify regional brain volumes.[12] Brain volume may mediate brain reserve which promotes the resilience of large-scale brain networks and helps maintain normal function in the face of neurodegeneration.[13-16] Previous studies have shown that subcortical volume loss reflects clinical measures of disease severity and is related to the development of cognitive impairment.[17-21] These studies raise the intriguing possibility that T1-weighted MRI measures of brain volume could be leveraged to identify biotypes of PD. Critically, such PD biotypes defined by brain volume at diagnosis may predict disease progression, which may be advantageous in helping to determine prognosis and identify subgroups for clinical trials. Uribe and colleagues obtained cortical thinning patterns through

cluster analysis in nondemented PD with limited sampling of patients, showing different PD cortical thinning subtypes. These PD subtypes also showed different cortical thinning progression over time, but the difference between motor symptoms and the rates of disease progression of the different subtypes were not reported.[22] Severity and rate of disease progression are an important issue in PD therapeutics, and identifying progression biotypes of PD at diagnosis using neuroanatomical patterns may be one way to address heterogeneity in PD.

In this study, we used data-driven clustering approaches to identify neuroanatomical biotypes in early PD patients in the Parkinson's Progression Markers Initiative (PPMI, http://www.ppmi-info.org) database[23] based on the neuroanatomical pattern derived by deformation-based morphometry (DBM).[24] DBM is based on non-linear and intensity-based registration procedures that spatially normalize the entire brain to a standard template.[24] DBM does not assume the distributions of gray matter or white matter and preserves the entirety of the MRI data. PD involves axonal degeneration and neuronal cell death, with the latter being indexed by grey matter atrophy which is a relatively late event in the pathogenesis of PD.[25] Moreover neurodegeneration in PD initially preferentially affects subcortical regions through a purported disease-spreading process.[26] A particularly strong aspect of the DBM method is that it enables the detection of subcortical neuroanatomical features,[27] and previous studies have shown that DBM can detect morphological tissue changes in early-stage PD patients.[19] As such, DBM is particularly suitable for PD biotype discovery, compared to cortical thinning patterns and voxel-based morphometry (VBM). We hypothesize that if heterogeneity in clinical symptoms reflects true neuroanatomical biotypes of PD, then such neuroanatomical biotypes should be detectable in early disease, and might predict the type of symptoms or disease progression that a patient will develop. The aim of our study was to: (1) identify biotypes of PD with cluster analysis based on a baseline neuroimaging dataset; (2) introduce a practical clinical typing method, which assigns individual patients to their biotype; (3) compare the behavioral assessments and rate of disease progression between different PD biotypes.

Materials and methods

Overall design

A flow chart of the analysis is shown in figure 1. We began by designing and implementing a preprocessing procedure to control for site- and age-related effects in a multisite data set that comprised structural MRI scans for 457 subjects (n = 314 patients with PD; n = 143 healthy controls). A graphical summary of the participants selection is shown in data available from Dryad (figure e-1): doi.org/10.5061/dryad.xsj3tx9bf. Patients and controls were matched for

age and sex. DBM was used to detect the volume of each voxel, compared to the template brain.[24] Next, to select features for use in clustering, we used Spearman rank correlation analysis to identify a low-dimensional representation of neuroanatomical features that were associated with baseline clinical symptoms within PD patients, including MDS-UPDRS parts I, II, III, Tremor and PIGD scores. To capture more neuroanatomical features related to PD, correlations were not corrected for multiple comparisons, but the dimensions of selected features were further reduced by principal components analysis (PCA). Then, hierarchical clustering was used to discover clusters of patients based on the principal components. Finally, in order to validate the clustering results, we investigated differences in follow-up clinical symptoms and neuroanatomical patterns between sub-groups of patients, and also investigated the extent to which the analysis could reliably discriminate between different sub-groups of patients using a pattern classification approach.

Study setting and patients

The Parkinson's Progression Markers Initiative (PPMI, http://www.ppmi-info.org) is a landmark observational, longitudinal database consisting of neuroimaging, biological tests and clinical and behavioral assessments in over 400 *de novo* PD patients.[23] All patients underwent dopamine transporter (DAT) imaging and the diagnosis was confirmed by the DAT deficit. All clinical features were reassessed annually over five years, so that markers of disease progression can be discerned. The neuroimaging data and extensive longitudinal clinical information provides an unprecedented opportunity to identify the neuroanatomical biotypes of PD, and the longitudinal assessment of PD progression of different biotypes in *de novo* PD patients. The clinical and behavioral assessments have been extensively described elsewhere.

Recruitment criteria included: age > 30 years, PD diagnosis within the last 2 years, baseline Hoehn and Yahr Stage I–II, and no anticipated need for symptomatic treatment within 6 months of baseline.[23] Clinical assessments were performed at baseline and at 3 months intervals during the first year of participation and then every 6 months thereafter (see data available from Dryad, table e-1, doi.org/10.5061/dryad.xsj3tx9bf). Data from the PPMI database were obtained in May 2018 in compliance with the PPMI Data Use Agreement.

Baseline and clinical assessments

A comprehensive set of clinical assessments were assessed in PPMI. We focused on clinical features that capture major PD symptoms, including both motor and non-motor symptoms, in line with previous studies.[3, 7, 28, 29] Details of clinical assessments used in this study are presented in PPMI (http://www.ppmi-info.org/wp-content/uploads/2010/04/PPMI-General-Operations-Manual.pdf). Derived variable definitions and score calculations are available in the PPMI (in the

Study_Docs). A list of abbreviations of clinical assessments are shown in data available from Dryad (table e-2): doi.org/10.5061/dryad.xsj3tx9bf. Features captured include:

(1) Demographics: age, sex, race, symptom duration, education level.

(2) Blood biomarkers: biochemical tests.

(3) Motor: Movement Disorder Society-Sponsored Revision of the Unified Parkinson's Disease Rating Scale (MDS-UPDRS)-Part I, MDS-UPDRS-Part II, MDS-UPDRS-Part III,[30] tremor/ PIGD motor phenotype, postural instability and gait disorder (PIGD) score, Tremor subscale, Schwab-England activities of daily living (ADL) score (Schwab & England ADL).

(4) Cognitive testing: cognitive function [age/education adjusted Montreal Cognitive Assessment total score (MoCA)][31], and neuropsychological variables including Visuospatial and visuoperceptual functions [Benton Judgment of Line Orientation (JOLO)][32], cognition performance [Symbol Digit Modalities Test (SDMT)][33], verbal learning and memory [Hopkins Verbal Learning Test (HVLT) for total recall, delayed recall, retention and recognition-discrimination][34], semantic memory [Semantic Verbal Fluency (SVF) test] [34] and working memory capacity [letter-number sequencing (LNS)][35].

(5) Autonomic testing: autonomic dysfunction [Scales for Outcomes in Parkinson's disease-Autonomic (SCOPA-AUT) total score and its sub scores: cardiovascular, constipation, orofacial, thermoregulatory, sexual, pupillo-motor and urinary][36].

(6) Sleep disorders: REM sleep behavior disorder (RBD) [RBD screening questionnaire (RBDSQ)][37], average sleep propensity in daily life (ASP) [Epworth Sleepiness Score (ESS)] [38].

(7) NeuroBehavior: depression [Geriatric Depression Scale (GDS) score][39], trait and state anxiety [State-Trait Anxiety Inventory (STAI) score][29], and impulse control disorders and related disorders [Questionnaire for Impulsive-Compulsive Disorders in Parkinson's disease (QUIP) score][40].

(8) Olfactory testing: impaired olfaction [age/sex adjusted University of Pennsylvania Smell Identification Test (UPSIT) score][41].

(9) Physical Activity: Physical Activity Scale of the Elderly (PASE).[42] Three activity categories were assessed in the PASE: leisure, household chores, and work/volunteering.

CSF and SPECT biomarkers

The lumbar puncture (LP) was conducted for all subjects for the collection of cerebral spinal fluid (CSF). Amyloid-beta1–42 (Aβ1–42), phosphorylated tau (P-tau) and total Tau protein (t-Tau) were measured by INNO-BIA AlzBio3 immunoassay (Innogenetics Inc.), and alpha-synuclein concentration (α-syn) was measured by enzyme-linked immunosorbent assay. Single-photon emission computed tomography (SPECT) with the DAT tracer ^{123}I-ioflupane was acquired at baseline and follow-up visits.[23]

Imaging Processing

T1-weighted MRI scan acquisition parameters are detailed in (http://www.ppmi-info.org/wp-content/uploads/2017/06/PPMI-MRI-Operations-Manual-V7.pdf).

3T high-resolution T1 structural images were preprocessed by using the Computational Anatomy Toolbox (CAT 12) (http://dbm.neuro.uni-jena.de/cat12/), which is an extension to SPM12 to provide computational anatomy. All these images were corrected for bias, noise and intensity, and linearly and then non- linearly registered to the MNI-152-2009c template. Then the deformation-based morphometry (DBM) (i.e. the determinant of the Jacobian transformation matrix) maps were calculated to estimate the local volume in each voxel (DBM values). Raw images of lower quality (CAT Image Quality Rating below 75%) were excluded. The rest images were further visually checked. Finally, the obtained preprocessed volume-based DBM data from 314 PD patients and 145 healthy controls (HC) were smoothed with an 8 mm full width at half maximum.

For volumetric analysis, FreeSurfer V5.3 was used to derive measures of the volume of subcortical nuclei. This is a well-documented and freely available software.[12]

Voxel-level association study and clustering

We reasoned that a low-dimensional representation of a subset of neuroanatomical features would best characterize biologically meaningful PD biotypes, similar to the atrophy subtypes detected in prodromal Alzheimer's disease.[11] Therefore, to select a set of neuroanatomical features for use in clustering, we used Spearman's rank correlation analysis to identify features that were significantly correlated ($P < 0.01$) with clinical scores (baseline value): the MDS-UPDRS-Part I-III, UPDRS-total, tremor score and PIGD score. Confounding factors like age, gender, years of education, race (categorized as white or other) and site effect were regressed out before feature selection.

To further exclude undesired background noise, principal component analysis (PCA) was used to extract a lower dimensional component space of the selected features (79 principal components were used capturing 90% of the variance). Then we used hierarchical clustering to assign subjects to nested subgroups with similar pattern. We calculated a similarity matrix describing the correlation distance between every pair of subjects, and then used Ward's minimum variance method to iteratively link pairs of subjects in closest proximity, forming progressively larger clusters in a hierarchical tree. Calinski-Harabasz criterion values were

used to estimate the optimal number of clusters, and the result suggested two clusters as the best choice (see data available from Dryad, figure e-2, doi.org/10.5061/dryad.xsj3tx9bf). Furthermore, to validate the clustering, we also clustered data using k-means clustering. The Cohen's Kappa agreement rate between hierarchical clustering and k-means clustering was 0.68, which is in the substantial range, suggesting that the patterns identified by the two different clustering methods were similar (see data available from Dryad, figure e-3, doi.org/10.5061/dryad.xsj3tx9bf).

Classification

To further test the clinical relevance of the identified neuroanatomical features as diagnostic features of biotypes, we applied a support vector machine (SVM) to test how well this could discriminate these two biotypes, that is, classify individuals into one of these two subgroups. A 10-kfold cross-validation strategy was used to estimate its accuracy, sensitivity and specificity. The details of classification are depicted in data available from Dryad (figure e-4): doi.org/10.5061/dryad.xsj3tx9bf.

Statistical analyses

Demographics and clinical variables

The t-test was used to determine the statistical significance of continuous demographic and clinical variables after removing confounding variables: age, gender, years of education, race (categorized as white or other) and site effect. The $\chi 2$ test was used to test the significance of categorical demographic variables and phenotype variables. Statistical significance was established at $P < 0.05$ (FDR correction) and the values were reported as mean (SD) for each demographic and clinical variable. Missing data were not included in all analysis.

Linear mixed model fitting for disease progression rates

We estimated rates of progression for each patient with five years of follow up. Linear mixed models were used to evaluate baseline and disease progression rates over time in patients classified in the subtypes using the 'lme4' package in R.[43] Gender, age, sites, race, time from baseline (months), biotype, and their interaction were included as fixed effects. Subject intercepts and slopes (rates of progression) were modelled as random effects.

Standard Protocol Approvals, Registrations, and Patient Consents

The study was approved by the institutional review board at each PPMI site. Written informed consent for research was obtained from all participants in the study.

Data Availability

All deidentified clinical and imaging data are available on the PPMI website (http://www.ppmi-info.org) and from the corresponding author on reasonable request.

Results

Baseline dataset characteristics

A total of 314 early PD patients were included in this study consisting of 207 (65.9%) males and 107 (34.1%) females. On average, these PD patients were 61.0 ± 9.5 years old with disease duration (date of enrollment minus the date of diagnosis) of 6.9 ± 6.8 months at baseline. The mean MDS-UPDRS parts I, II and III scores were 5.6 ± 4.0, 5.9 ± 4.2 and 20.7 ± 8.7, respectively. Clinical, biological and cognitive characteristics of early PD patients and matched healthy controls can be found in table 1.

The neuroanatomical features associated with the symptoms of Parkinson's disease

Figure 2 shows the correlation analysis between deformation values and baseline clinical scores. We found that there were a number of neuroanatomical features that correlated with UPDRS scores, including areas spanning the caudate, putamen, thalamus, hippocampus, supplementary motor area and orbital frontal gyrus (figure 2). These areas are consistent with previous findings that subcortical volume loss correlates with motor symptom severity.[18] This empirical, data-driven approach to feature selection identified 23213 voxel's DBM values that were correlated with at least one baseline clinical score (figure 2).

Brain neuroanatomical patterns define two Parkinson's disease biotypes

We then tested whether these neuroanatomical feature sets tended to cluster in patient subgroups. As illustrated in figure 3 and data available from Dryad (figure e-3): doi.org/10.5061/dryad.xsj3tx9bf, the cluster analysis revealed two distinct clusters of PD patients, with similar disease duration (P = 0.35, table 1). These two clusters comprised 36.31% (114 patients) and 63.69% (200 patients) of the 314 patients with PD, respectively. Table 1 shows the demographic characteristics of the two biotype groups. There was no significant difference in age, sex, education, symptom duration or in the ratio of PIGD and tremor dominant patients between the two biotype groups (table 1and data available from Dryad, table e-3, doi.org/10.5061/dryad.xsj3tx9bf).

Neuroanatomical pattern of the two biotypes

To illustrate the neuroanatomical pattern in the different PD biotypes, the DBM values of the two biotypes was compared with controls. Compared to normal controls, both biotypes showed significant differences in subcortical regions. Figure 4 shows the comparison between each biotype with healthy controls ($P < 0.005$, FDR correction).

Biotype 1 had pronounced differences compared to normal controls in almost the whole brain, indicating more severe atrophy in brain areas in early PD. Biotype 2 had predominant differences in the subcortical regions. In addition, we found other distinct patterns that differentiated the two biotypes. For example, as compared to controls DBM values in putamen, caudate, pallidum, lingual gyrus, temporal cortex, insula, amygdala, hippocampus and orbital frontal cortex, which regulate motor-related, cognitive and emotional related behavior, were significantly lower in biotype 1 patients, which were characterized in part by increased motor and non-motor symptom scores. In contrast, biotype 2 patients had significantly higher DBM values in the brainstem, putamen, caudate, occipital lobe, lingual gyrus, olfactory, posterior cingulate cortex, and white matter areas compared to controls. Additional volumetric analyses using FreeSurfer showed biotype 1 patients had significantly lower subcortical volumes within the thalamus, caudate, putamen, pallidum, accumbens, amygdala and hippocampus ($P < 0.05$, FDR correction), as compared to biotype 2 patients (see data available from Dryad, table e-4, doi.org/10.5061/dryad.xsj3tx9bf).

Neuroanatomical patterns for diagnosing Parkinson's disease biotypes

We reasoned that clustering could be used for training the classifiers for the diagnosis of PD biotypes solely on the basis of structural MRI measures. To this end, we trained classifiers for predicting the PD biotype in individual patients. Ten-fold cross-validation was used to assess performance and significance. Support-vector machine (SVM) classifiers (using Gaussian kernel functions) yielded overall accuracy rates of 84.1% (Sensitivity: 0.71, Specificity: 0.89, AUC: 0.90, see data available from Dryad, figure e-6, doi.org/10.5061/dryad.xsj3tx9bf) for the clusters characterized above.

Baseline differences in symptoms between biotypes

Table 1 shows that at baseline biotype 1 had worse mentation, behavior and mood (higher MDS-UPDRS Part I score) and very much worse REM Sleep Behavior Disorder (RBD score) than biotype 2. There was also evidence of more severe autonomic function in the biotype 1 (SCOPA total score) (table 1).

Disease progression in the Parkinson's disease biotypes

The PPMI patients were followed for five years. The sample size of the progression analysis is shown in data available from Dryad (table e-1): doi.org/10.5061/dryad.xsj3tx9bf. Results from a linear mixed model showed that the biotype 1 had significantly greater progression in all MDS-UPDRS scores, with the exception of the tremor score (figure 5 and table 2). In addition, biotype 1 also tended to develop more severe cognitive impairment (HVLT immediate total recall, Letter number sequencing and Symbol Digit Modalities) (table 2 and

data available from Dryad, figure e- 8, doi.org/10.5061/dryad.xsj3tx9bf**)**. More rapid progression could also be seen in the biotype 1 in activities of daily living (Schwab & England ADL) (table 2 and data available from Dryad, figure e- 7, doi.org/10.5061/dryad.xsj3tx9bf).

On dopaminergic SPECT scanning, biotype 1 had worse denervation of both left caudate and left putamen after an average of four years of follow-up. The right caudate and right putamen showed no significant difference in denervation between the two biotypes (see data available from Dryad, figure e-13, doi.org/10.5061/dryad.xsj3tx9bf).

To summarize, biotype 1 had higher baseline MDS-UPDRS I, worse baseline sleep problems and autonomic dysfunction, and faster progression of most motor symptoms, cognitive impairment and activities of daily living, compared to biotype 2 (all $P < 0.05$, FDR correction) (figure 5 and table 1,2).

Discussion

In this study, we identified two neuroanatomical biotypes in PD patients with otherwise similar demographics using an unbiased data-driven clustering approach applied to the PPMI cohort. Neuroanatomical biotypes differed in symptomatology even at presentation before treatment, and thereafter progressed at different rates. The most striking baseline difference was the much higher REM Sleep Behavior Disorder screening questionnaire score in biotype 1.

Pathophysiological explanations

Our results provide support for two different neuroanatomical phenotypes within PD patients. Compared to healthy controls, the neuroanatomical differences were more widespread in patients with biotype 1, spanning across almost all of the brain. Compared to patients with biotype 1, patients with biotype 2 had less widespread differences at baseline.

Biotype 2 patients had larger subcortical volume (higher DBM values) than controls on average, suggesting they may contain more cells (including dopaminergic cells) and synapses, increasing the ability to support maintenance of function despite declines in brain volume. Accordingly, biotype 2 patients had a slower disease progression rate.[3] In contrast, biotype 1 patients had less brain reserve, and did not compensate as well as PD progressed over time resulting in a faster disease progression rate. Indeed, there was evidence that this was already the case at the time of presentation, given the worse symptom severity in several domains in

biotype 1 than in biotype 2. In summary, we hypothesize that the different rates of symptom progression relate to different brain reserves.[13, 16]

Brain reserve describes the differences in brain volume and structure that may support maintenance of function despite pathology.[13, 44] Gross or regional brain volume reflects the quantity of neurons, neuronal integrity and synaptic densities, which determine the brain's ability to engage in compensatory activity.[13, 44] Prior works have highlighted a link between brain volume and markers of functional reserve in patients with Parkinson's disease and other neurodegenerative diseases.[14-16] For example, there is a relationship between brain grey matter volume and the magnitude of network-level integration.[16] Basal forebrain volume can predict future psychosis in early Parkinson's disease and higher cholinergic nucleus 4 gray matter density is associated with a lower risk of reporting psychotic symptoms.[17] PD with cognitive impairment shows lower grey matter volume in the nucleus basalis of Meynert.[20] Compared to TD patients, PIGD patients had lower gray matter volumes in the globus pallidus and amygdala, and PIGD patients have worse prognosis with a more rapid decline.[45, 46] In line with these observations, our results suggest that a larger subcortical volume helps limit the negative impact of PD pathology during disease progression, as represented by brain atrophy. Physical exercise has been shown to increase brain volume in older adults[47], and therefore interventions that increase physical activity before or in the early course of PD may contribute to brain reserve and help slow down rates of disease progression.

Distinct patterns of longitudinal progression

At baseline, biotype 1 had evidence of worse behavioral, autonomic and motor impairment, and above all, of worse RBD symptomatology. These findings are consistent with past observations, showing that motor dysfunction is associated with cognitive decline, autonomic dysfunction and RBD.[28, 48] PD with RBD is also associated with faster motor progression and higher risk of cognitive decline.[28] In line with these studies, we found biotype 1 had very much worse RBD symptomatology and more cognitive decline. RBD may be a useful marker for early subtyping of Parkinson's disease at baseline.[28] Biotype 1 patients had significantly higher scores in several motor disease symptoms, after only one year's follow-up, but there was no difference in the progression of tremor between the two biotypes. This may reflect that rest tremor may be more closely related to degeneration of non-dopaminergic, rather than dopaminergic, systems.[49] In most cases there is a substantial asymmetry of clinical symptoms from disease onset, and patients with unilateral disease showed a significant difference in striatal uptake between the ipsilateral and contralateral sides in both the caudate and putamen nuclei.[49] Differences in longitudinal denervation between the left and right caudate and putamen between the two biotypes (see data available from Dryad, figure e-12, doi.org/10.5061/dryad.xsj3tx9bf) may reflect different disease severity. Consistent with previous findings that CSF biomarkers are not useful biomarkers of PD progression,[50] our

results didn't observe significant differences in CSF biomarker levels between the two biotypes at baseline (table 1).

Limitations and applications

While the two identified neuroanatomical biotypes showed group differences in terms of symptom severity and longitudinal progression, there is overlap in the clinical scores at the individual level between the two biotypes. It is plausible that some patients were a combination of more than one biotype, and this would not be captured by our approach of discretizing biotypes. Future research should further investigate more refined biotype definitions based on continuous membership probability values through longitudinal studies in larger cohorts. Therefore, we regard the two biotypes identified here as just an initial solution to the problem of diagnostic heterogeneity in a subtyping process that relies primarily on neuroanatomical features correlated with clinical scores. It is likely that cohort limitations (the PPMI patients on the whole have higher level of education, are younger and have less baseline disability than the general PD population[23]), the size of our cluster-discovery data set, and the subjectivity of clinical-symptom assessments were also limiting factors. For these reasons, a novel cohort with longitudinal clinical data will be useful for validating the present findings.

We show that neuroanatomical biotypes can be defined that robustly predict different rates of progression, suggesting that these reflect true biotypes of PD. Given that PPMI recruited early patients from multiple sites, our results should still be mostly generalizable to early PD in real clinical practice where the findings can be used to inform estimates of prognosis. These results might also have implications for clinical trial design in early PD in the future. The existence of neuroanatomical biotypes that show specific trajectories of clinical score decline may require biotype-specific outcome measures tailored to the expected rate of decline in different domains.

Conclusion

In conclusion, we have robustly identified two different neuroanatomical biotypes amongst early PD patients using a data-driven clustering approach. These biotypes showed distinct neuroanatomical patterns, symptoms and rates of progression. Recognition of this heterogeneity is an important step towards precision medicine for PD.

Appendix 1: Authors

Name	Location	Contribution
Linbo Wang, PhD	Fudan University	Data curation, Software, Formal analysis, Investigation, Visualization, Methodology, Writing—original draft, Writing—review and editing
Wei Cheng, PhD	Fudan University	Resources, Data curation, Conceptualization, Formal analysis, Supervision, Investigation, Methodology, Project administration, Writing-review and editing
Edmund Rolls, DPhil, DSc	University of Oxford	Conceptualization, Interpreted the data, Methodology, revised the manuscript for intellectual content
Fuli Dai, MSc	Fudan University	Resources, Data curation, Methodology
Weikang Gong, PhD	Fudan University	Resources, Data curation, Software, Methodology
Jingnan Du, MSc	Fudan University	Resources, Data curation, Software, Methodology
Wei Zhang, BSc	Fudan University	Data curation, Software, Methodology
Shouyan Wang, PhD	Fudan University	Interpreted the data; revised the manuscript for intellectual content
Fengtao Liu, MD	Fudan University	Interpreted the data; revised the manuscript for intellectual content
Jian Wang, MD	Fudan University	Interpreted the data; revised the manuscript for intellectual content
Peter Brown, MD	University of Oxford	Supervision, Investigation, Methodology, Project administration, Writing—review and editing.
Jianfeng Feng, PhD	Fudan University	Conceptualization, Resources, Supervision, Funding acquisition, Investigation, Methodology, Project administration, Writing—review and editing.

References

1. Schapira AHV, Chaudhuri KR, Jenner P. Non-motor features of Parkinson disease. Nat Rev Neurosci 2017;18:435-450.
2. Fereshtehnejad SM, Postuma RB. Subtypes of Parkinson's Disease: What Do They Tell Us About Disease Progression? Curr Neurol Neurosci Rep 2017;17:34.
3. Fereshtehnejad S-M, Zeighami Y, Dagher A, Postuma RB. Clinical criteria for subtyping Parkinson's disease: biomarkers and longitudinal progression. Brain 2017;140:1959-1976.
4. Fereshtehnejad S-M, Romenets SR, Anang JBM, Latreille V, Gagnon J-F, Postuma RB. New Clinical Subtypes of Parkinson Disease and Their Longitudinal Progression. JAMA Neurology 2015;72:863-873.
5. Lewis SJG, Foltynie T, Blackwell AD, Robbins TW, Owen AM, Barker RA. Heterogeneity of Parkinson's disease in the early clinical stages using a data driven approach. Journal of Neurology Neurosurgery and Psychiatry 2005;76:343-348.
6. Xu X, Chan P. Clinical subtypes of Parkinson's disease based on nonmotor symptoms: A cluster analysis. Movement Disorders 2018;33:S725-S725.
7. Zhang X, Chou J, Liang J, et al. Data-Driven Subtyping of Parkinson's Disease Using Longitudinal Clinical Records: A Cohort Study. Sci Rep 2019;9:797.
8. De Pablo-Fernández E, Lees AJ, Holton JL, Warner TT. Prognosis and Neuropathologic Correlation of Clinical Subtypes of Parkinson Disease. JAMA Neurology 2019;76.
9. Erro R, Picillo M, Vitale C, et al. Clinical clusters and dopaminergic dysfunction in de-novo Parkinson disease. Parkinsonism & Related Disorders 2016;28:137-140.
10. Mestre TA, Eberly S, Tanner C, et al. Reproducibility of data-driven Parkinson's disease subtypes for clinical research. Parkinsonism Relat Disord 2018;56:102-106.
11. Ten Kate M, Dicks E, Visser PJ, et al. Atrophy subtypes in prodromal Alzheimer's disease are associated with cognitive decline. Brain 2018;141:3443-3456.
12. Fischl B, Salat DH, Busa E, et al. Whole brain segmentation: automated labeling of neuroanatomical structures in the human brain. Neuron 2002;33:341-355.
13. Gregory S, Long JD, Kloppel S, et al. Operationalizing compensation over time in neurodegenerative disease. Brain 2017;140:1158-1165.
14. Guo LH, Alexopoulos P, Wagenpfeil S, Kurz A, Perneczky R, Alzheimer's Disease Neuroimaging I. Brain size and the compensation of Alzheimer's disease symptoms: a longitudinal cohort study. Alzheimers Dement 2013;9:580-586.
15. Gregory S, Long JD, Kloppel S, et al. Testing a longitudinal compensation model in premanifest Huntington's disease. Brain 2018;141:2156-2166.
16. Shine JM, Bell PT, Matar E, et al. Dopamine depletion alters macroscopic network dynamics in Parkinson's disease. Brain 2019;142:1024-1034.
17. Barrett MJ, Blair JC, Sperling SA, Smolkin ME, Druzgal TJ. Baseline symptoms and basal forebrain volume predict future psychosis in early Parkinson disease. Neurology 2018;90:e1618-e1626.
18. Wilson H, Niccolini F, Pellicano C, Politis M. Cortical thinning across Parkinson's

disease stages and clinical correlates. J Neurol Sci 2019;398:31-38.
19. Borghammer P, Østergaard K, Cumming P, et al. A deformation-based morphometry study of patients with early-stage Parkinson's disease. European Journal of Neurology 2010;17:314-320.
20. Schulz J, Pagano G, Fernandez Bonfante JA, Wilson H, Politis M. Nucleus basalis of Meynert degeneration precedes and predicts cognitive impairment in Parkinson's disease. Brain 2018;141:1501-1516.
21. Zeighami Y, Fereshtehnejad SM, Dadar M, et al. A clinical-anatomical signature of Parkinson's disease identified with partial least squares and magnetic resonance imaging. Neuroimage 2019;190:69-78.
22. Uribe C, Segura B, Baggio HC, et al. Progression of Parkinson's disease patients' subtypes based on cortical thinning: 4-year follow-up. Parkinsonism Relat Disord 2019.
23. Parkinson Progression Marker I. The Parkinson Progression Marker Initiative (PPMI). Prog Neurobiol 2011;95:629-635.
24. Chung MK, Worsley KJ, Paus T, et al. A unified statistical approach to deformation-based morphometry. Neuroimage 2001;14:595-606.
25. Lanskey JH, McColgan P, Schrag AE, et al. Can neuroimaging predict dementia in Parkinson's disease? Brain 2018;141:2545-2560.
26. Pandya S, Zeighami Y, Freeze B, et al. Predictive model of spread of Parkinson's pathology using network diffusion. Neuroimage 2019;192:178-194.
27. Scanlon C, Mueller SG, Tosun D, et al. Impact of methodologic choice for automatic detection of different aspects of brain atrophy by using temporal lobe epilepsy as a model. AJNR Am J Neuroradiol 2011;32:1669-1676.
28. Pagano G, De Micco R, Yousaf T, Wilson H, Chandra A, Politis M. REM behavior disorder predicts motor progression and cognitive decline in Parkinson disease. Neurology 2018;91:e894-e905.
29. Kendall PC, Finch AJ, Jr., Auerbach SM, Hooke JF, Mikulka PJ. The State-Trait Anxiety Inventory: a systematic evaluation. J Consult Clin Psychol 1976;44:406-412.
30. Goetz CG, Tilley BC, Shaftman SR, et al. Movement Disorder Society-sponsored revision of the Unified Parkinson's Disease Rating Scale (MDS-UPDRS): scale presentation and clinimetric testing results. Mov Disord 2008;23:2129-2170.
31. Nasreddine ZS, Phillips NA, Bedirian V, et al. The Montreal Cognitive Assessment, MoCA: a brief screening tool for mild cognitive impairment. J Am Geriatr Soc 2005;53:695-699.
32. Benton AL, Varney NR, Hamsher KD. Visuospatial judgment. A clinical test. Arch Neurol 1978;35:364-367.
33. Forn C, Belloch V, Bustamante JC, et al. A symbol digit modalities test version suitable for functional MRI studies. Neurosci Lett 2009;456:11-14.
34. Shapiro AM, Benedict RH, Schretlen D, Brandt J. Construct and concurrent validity of the Hopkins Verbal Learning Test-revised. Clin Neuropsychol 1999;13:348-358.
35. Christensen BK, Girard TA, Bagby RM. Wechsler Adult Intelligence Scale-Third Edition short form for index and IQ scores in a psychiatric population. Psychol Assess

2007;19:236-240.
36. Visser M, Marinus J, Stiggelbout AM, Van Hilten JJ. Assessment of autonomic dysfunction in Parkinson's disease: the SCOPA-AUT. Mov Disord 2004;19:1306-1312.
37. Stiasny-Kolster K, Mayer G, Schafer S, Moller JC, Heinzel-Gutenbrunner M, Oertel WH. The REM sleep behavior disorder screening questionnaire--a new diagnostic instrument. Mov Disord 2007;22:2386-2393.
38. Johns MW. A new method for measuring daytime sleepiness: the Epworth sleepiness scale. Sleep 1991;14:540-545.
39. Yesavage JA. Geriatric Depression Scale. Psychopharmacol Bull 1988;24:709-711.
40. Weintraub D, Hoops S, Shea JA, et al. Validation of the questionnaire for impulsive-compulsive disorders in Parkinson's disease. Mov Disord 2009;24:1461-1467.
41. Doty RL, Shaman P, Kimmelman CP, Dann MS. University of Pennsylvania Smell Identification Test: a rapid quantitative olfactory function test for the clinic. Laryngoscope 1984;94:176-178.
42. Washburn RA, Smith KW, Jette AM, Janney CA. The Physical Activity Scale for the Elderly (PASE): development and evaluation. J Clin Epidemiol 1993;46:153-162.
43. Lamprianou I. Application of single-level and multi-level Rasch models using the lme4 package. J Appl Meas 2013;14:79-90.
44. Gregory S, Long JD, Tabrizi SJ, Rees G. Measuring compensation in neurodegeneration using MRI. Curr Opin Neurol 2017;30:380-387.
45. Rosenberg-Katz K, Herman T, Jacob Y, Kliper E, Giladi N, Hausdorff JM. Subcortical Volumes Differ in Parkinson's Disease Motor Subtypes: New Insights into the Pathophysiology of Disparate Symptoms. Front Hum Neurosci 2016;10:356.
46. Rosenberg-Katz K, Herman T, Jacob Y, Giladi N, Hendler T, Hausdorff JM. Gray matter atrophy distinguishes between Parkinson disease motor subtypes. Neurology 2013;80:1476-1484.
47. Erickson KI, Voss MW, Prakash RS, et al. Exercise training increases size of hippocampus and improves memory. Proc Natl Acad Sci U S A 2011;108:3017-3022.
48. Wang YX, Zhao J, Li DK, et al. Associations between cognitive impairment and motor dysfunction in Parkinson's disease. Brain Behav 2017;7:e00719.
49. Djaldetti R, Ziv I, Melamed E. The mystery of motor asymmetry in Parkinson's disease. The Lancet Neurology 2006;5:796-802.
50. Parnetti L, Gaetani L, Eusebi P, et al. CSF and blood biomarkers for Parkinson's disease. Lancet Neurol 2019;18:573-586.

Table 1. The demographic, clinical and imaging characteristics of controls and Parkinson's disease biotype groups. The T values and *P* values are for the comparison between biotype 1 and biotype 2 PD patients. Baseline scores are presented, as well as the change over follow-up in the case of clinical measures, given as ∆(t2-t1)**.** Here t1 is score at baseline and t2 the score after five years follow-up. All values in brackets are standard deviation (SD) unless otherwise specified. The *P* values are FDR-corrected for multiple comparisons. Significant ($P < 0.05$)

	Biotype 1 PD		**Biotype 2 PD**		**T-vale**		***P*-value**	
Demography	**Baseline**	**∆(t2-t1)**	**Baseline**	**∆(t2-t1)**	**Baseline**	**∆(t2-t1)**	**Baseline**	**∆(t2-t1)**
Age at onset, years	61.6(8.6)		60.7(10)		-0.697		0.691	
Male sex (%)	76(0.7)		131(0.7)		0.044		0.901	
Education history, year	15.6(2.8)		15.5(3.2)		-1.298		0.47	
White race (%)	106(0.9)		187(0.9)		0.044		0.901	
Symptoms duration, month	7.3(7.5)		6.7(6.3)		-0.935		0.562	
UPDRS-Total score	33.92(13.9)	23.7(20.8)	30.86(12.6)	13.9(17.5)	-2.44	-2.00	0.147	0.178
Motor symptoms and signs								
UPDRS-Part II	6.3(4.36)	7.6(6.5)	5.63(4.11)	3.7(5.3)	-1.39	-3.06	0.455	0.029
UPDRS-Part III	21.14(8.94)	10.7(14.4)	20.11(8.63)	7.1(11.8)	-1.52	-1.3	0.39	0.38
Tremor score	0.46(0.27)	0.10(0.40)	0.49(0.31)	0(0.4)	0.68	-0.46	0.692	0.876
PIGD score	0.24(0.24)	0.04(0.60)	0.22(0.21)	0.2(0.3)	-1.11	-3.29	0.559	0.02
Schwab and England score	92.68(5.92)	-11.1(13)	93.95(5.46)	-7.1(9.3)	2.46	2.61	0.147	0.049
Tremor/PIGD phenotype (%)							0.347	
Tremor-dominant	76(67)		144(72)					
PIGD-dominant	17(15)		36(18)					
Intermediate	21(18)		20(10)					
Non-Motor symptoms and signs								
UPDRS-Part I	6.48(4.4)	5.4(5.1)	5.12(3.62)	3.2(5)	-3.34	-1.50	0.017	0.34
RBD score	5.07(2.99)	0.93(2.85)	3.69(2.3)	0.89(3.08)	-4.31	-0.28	0.001	0.903
Epworth Sleepiness Scale	6.1(3.4)	2.86(4.86)	5.8(3.6)	1.25(4.08)	-0.86	-2.30	0.585	0.085
Cognitive function								
MOCA (adjusted score)	27.12(2.1)	-1.41(4.66)	27.48(2.1)	-0.07(2.59)	1.06	2.95	0.559	0.031
Benton judgment of line orientation	12.5(2.2)	-0.96(2.51)	13(2)	-0.45(2.09)	2.19	1.45	0.147	0.34
HVLT immediate total recall	24.7(5.4)	-1.71(5.82)	24.5(4.7)	0.75(5.52)	-0.97	2.84	0.562	0.049
HVLT discrimination recognition	10.3(1.6)	0.41(1.99)	10.3(1.5)	0.66(2.11)	0.23	0.94	0.901	0.595
Hopkins verbal learning test	0.86(0.19)	0.008(0.316)	0.87(0.19)	0.02(0.25)	0.09	0.5	0.948	0.876

Letter number sequencing	10.4(2.6)	-1.19(2.66)	10.8(2.7)	-0.53(2.55)	0.63	1.44	0.698	0.34
Semantic Fluency	47.4(11)	-1.5(10.79)	49.1(10.9)	0.71(10.46)	1.15	1.40	0.54	0.34
Symbol Digit Modalities	40.7(9.1)	-4.77(10.89)	42.4(9.6)	-1.811(9.43)	1.26	1.89	0.473	0.204
SCOPA autonomic questionnaire								
Gastrointestinal	2.38(2.02)	2.31(2.19)	2(2.1)	1.48(2.54)	-1.32	-2.62	0.47	0.049
Urinary question	5.14(5.55)	1.47(9.15)	3.97(2.51)	1.19(2.6)	-2.31	-0.19	0.147	0.903
Cardiovascular	0.61(1.03)	0.44(1.33)	0.36(0.61)	0.40(1.06)	-2.61	-0.29	0.135	0.903
Thermoregulatory	1.24(1.54)	0.97(1.87)	1.09(1.3)	0.66(1.62)	-0.94	-1.17	0.562	0.453
Pupillomotor	0.45(0.72)	0.21(0.87)	0.39(0.68)	0.24(0.67)	-0.64	0.19	0.698	0.903
Sexual	4.7(6.4)	1.65(6.87)	3.2(5.7)	1.8117(6.68)	-2.25	-0.06	0.147	0.95
Total score	14.5(10.3)	7.27(13.36)	11.0(7.6)	5.79(8.99)	-3.35	-0.99	0.017	0.591
Geriatric Depression Scale	2.6(2.5)	0.5(2.48)	2.1(2.2)	0.68(2.86)	-2.15	0.31	0.147	0.903
State Trait Anxiety Inventory	33.3(9.8)	1.23(8.62)	31.5(9.1)	0.94(8.64)	-1.84	-0.22	0.315	0.903
STAI State Subscore	34.1(10.7)	-0.043(9.51)	32.1(9.8)	-0.68(10.52)	-1.57	-0.6	0.381	0.876
Impulse control disorders (QUIP scores)								
GMB	0.02(0.13)	0.029(0.168)	0.01(0.07)	-0.01(0.09)	-1.03	-1.51	0.559	0.34
SEX	0.04(0.21)	0.09(0.3)	0.02(0.12)	0.04(0.27)	-1.6	-0.45	0.371	0.876
EAT	0.05(0.22)	0.03(0.34)	0.01(0.1)	0.041(0.24)	-2.22	0.42	0.147	0.876
BUY	0.02(0.13)	0.03(0.17)	0.01(0.07)	-0.01(0.09)	-1.03	-1.51	0.559	0.34
Current Short	0.28(0.73)	0.17(0.99)	0.17(0.48)	0.11(0.79)	-1.61	-0.14	0.371	0.917
Other	0.15(0.45)	0(0.64)	0.13(0.38)	0.04(0.57)	-0.34	0.47	0.868	0.876
Olfaction UPSIT percentile	21.3(8.80)		23(1.30)		1.28		0.47	
Brain imaging								
Right Caudate	2(0.69)		1.97(0.51)		-0.33		0.868	
Left Caudate	1.92(0.68)		2.00(0.52)		1.35		0.47	
Right Putamen	0.85(0.39)		0.83(0.34)		0.10		0.948	
Left Putamen	0.77(0.37)		0.82(0.34)		1.72		0.347	
CSF biomarkers								
α-Synuclein	1431.02(564.96)		1506.34(689.83)		0.88		0.583	
Aβ42	880.5(322.85)		908.31(429.08)		0.42		0.848	
T-tau	165.12(53.4)		169.31(57.83)		0.49		0.805	
P-tau	14.35(4.76)		15(5.45)		0.79		0.628	
T-tau/Aβ42	0.203(0.095)		0.203(0.101)		0.03		0.976	
P-tau/Aβ42	0.017(0.01)		0.018(0.01)		0.39		0.859	
P-tau/T-tau	0.08(0.01)		0.09(0.01)		0.93		0.562	
Aβ42/α-synuclein	0.65(0.19)		0.64(0.23)		-0.30		0.878	
T-tau/α-synuclein	0.12(0.03)		0.12(0.03)		-0.96		0.562	
P-tau/α-synuclein	0.01(0.003)		0.01(0.002)		-0.18		0.905	

Table 2. Longitudinal motor and non-motor score estimated beta coefficients in different biotypes of Parkinson's disease with covariate correction in the PPMI patients with five years of follow-up. Annual changes were estimated from linear mixed models. Age, gender, race and sites were included as covariates. Values in brackets are standard deviation (SD). The *P* values are FDR-corrected for multiple comparisons. Significant ($P < 0.05$)

	Biotype 1	**Biotype 2**	**T-value**	***P*-value**
Total UPDRS score	5.32(0.39)	3.4(0.3)	3.92	<0.001
Motor symptoms and signs				
UPDRS-Part II	1.49(0.12)	0.81(0.09)	4.5	<0.001
UPDRS-Part III	2.6(0.25)	1.73(0.19)	2.76	0.025
Tremor score	0.022(0.008)	0.012(0.006)	0.99	0.485
PIGD score	0.111(0.011)	0.051(0.009)	4.2	0.001
Schwab and England score	-2.55(0.24)	-1.66(0.18)	-2.93	0.022
Non-Motor symptoms and signs				
UPDRS-Part I	1.22(0.1)	0.84(0.08)	2.91	0.022
RBD score	0.254(0.057)	0.225(0.043)	0.42	0.717
Epworth Sleepiness Scale	0.572(0.087)	0.384(0.066)	1.71	0.223
Cognitive function				
MOCA (adjusted score)	-0.268(0.07)	-0.09(0.053)	-2.02	0.121
Benton judgment of line orientation	-0.097(0.042)	-0.023(0.032)	-1.39	0.318
HVLT immediate total recall	-0.255(0.101)	0.11(0.077)	-2.86	0.024
HVLT discrimination recognition	0.061(0.041)	0.09(0.031)	-0.58	0.662
Hopkins verbal learning test	-0.013(0.005)	0.001(0.004)	-2.09	0.114
Letter number sequencing	-0.258(0.053)	-0.09(0.04)	-2.54	0.044
Semantic Fluency	-0.399(0.198)	0.016(0.15)	-1.67	0.226
Symbol Digit Modalities	-1.228(0.199)	-0.4(0.15)	-3.32	0.008
SCOPA autonomic questionnaire				
Gastrointestinal	0.409(0.048)	0.28(0.036)	2.15	0.106
Urinary question	0.271(0.087)	0.217(0.065)	0.49	0.708
Cardiovascular	0.096(0.021)	0.085(0.016)	0.43	0.717
Thermoregulatory	0.18(0.035)	0.133(0.027)	1.07	0.485
Pupillomotor	0.023(0.015)	0.042(0.011)	-1.03	0.485
Sexual	0.302(0.128)	0.431(0.097)	-0.8	0.582
Total score	1.269(0.19)	1.194(0.143)	0.32	0.776
Geriatric Depression Scale	0.17(0.055)	0.112(0.041)	0.85	0.572
State Trait Anxiety Inventory	0.249(0.343)	0.305(0.259)	-0.13	0.897
STAI State Subscore	-0.041(0.191)	0.098(0.144)	-0.58	0.662
QUIP scores				
GMB	0.005(0.003)	0(0.002)	1.44	0.314

SEX	0.012(0.005)	0.008(0.004)	0.67	0.662
EAT	0.006(0.005)	0.01(0.004)	-0.64	0.662
BUY	0.005(0.003)	0(0.002)	1.44	0.314
Other	0.027(0.01)	0.014(0.008)	1	0.485
Current Short	0.056(0.016)	0.032(0.012)	1.17	0.446

Figure legends

Figure 1. Schematic overview of the design of this study.

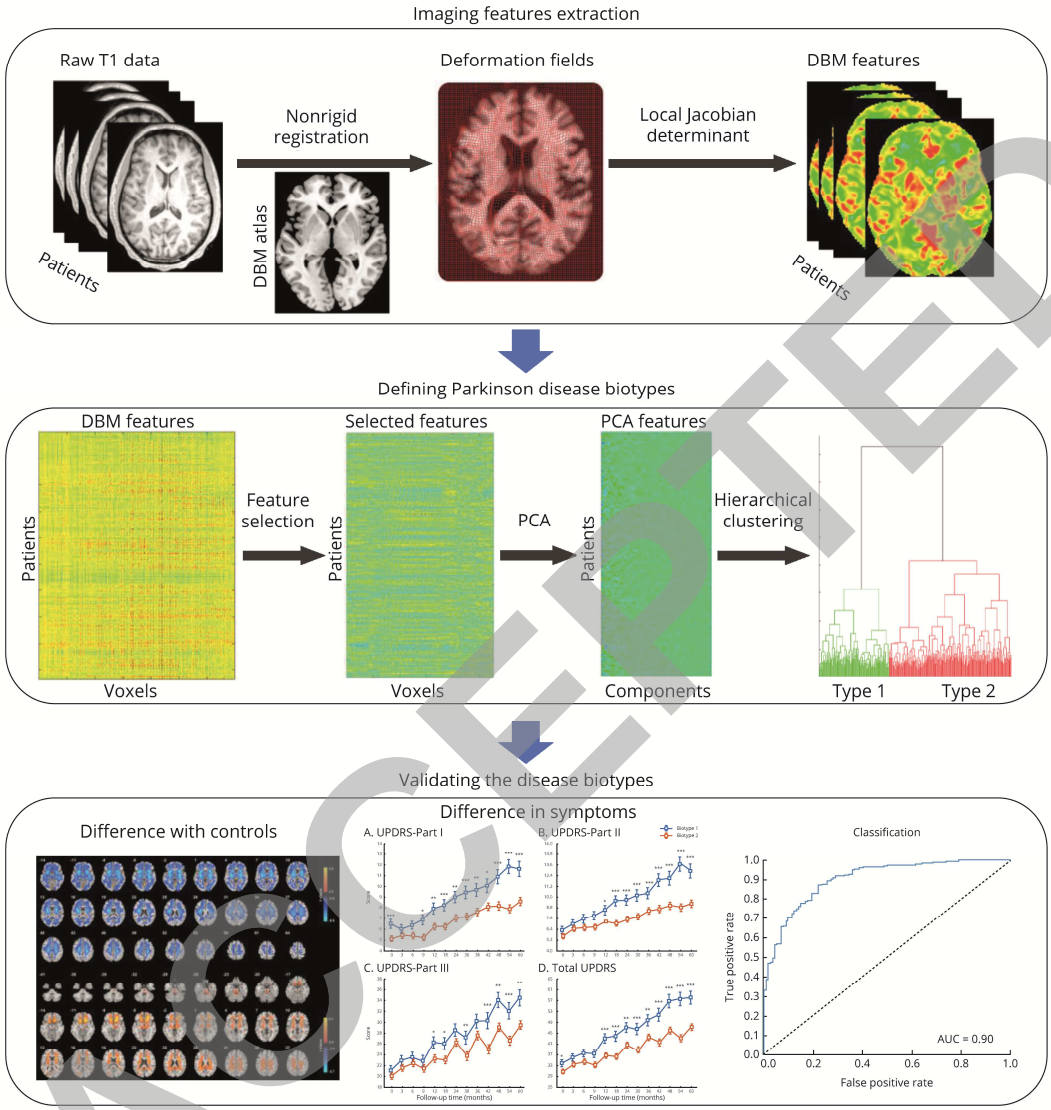

Figure 2. The correlation between DBM values and symptom scores. Warm color indicates a positive correlation between symptom scores and DBM values. Cold color indicates a negative correlation between symptom scores and DBM values. (A) The correlation between DBM values and MDS-UPDRS I score. (B) The correlation between DBM values and MDS-UPDRS II score. (C) The correlation between DBM values and MDS-UPDRS III score. (D) The correlation between DBM values and MDS-UPDRS total score. (E) The correlation between DBM values and the tremor score. (F) The correlation between DBM values and the PIGD score. 8855, 2826, 4201, 6064, 6994, 1380 deformation values correlated with UPDRS part I, UPDRS part II, UPDRS part III score, total UPDRS, PIGD score and tremor score, respectively ($P < 0.01$, uncorrected).

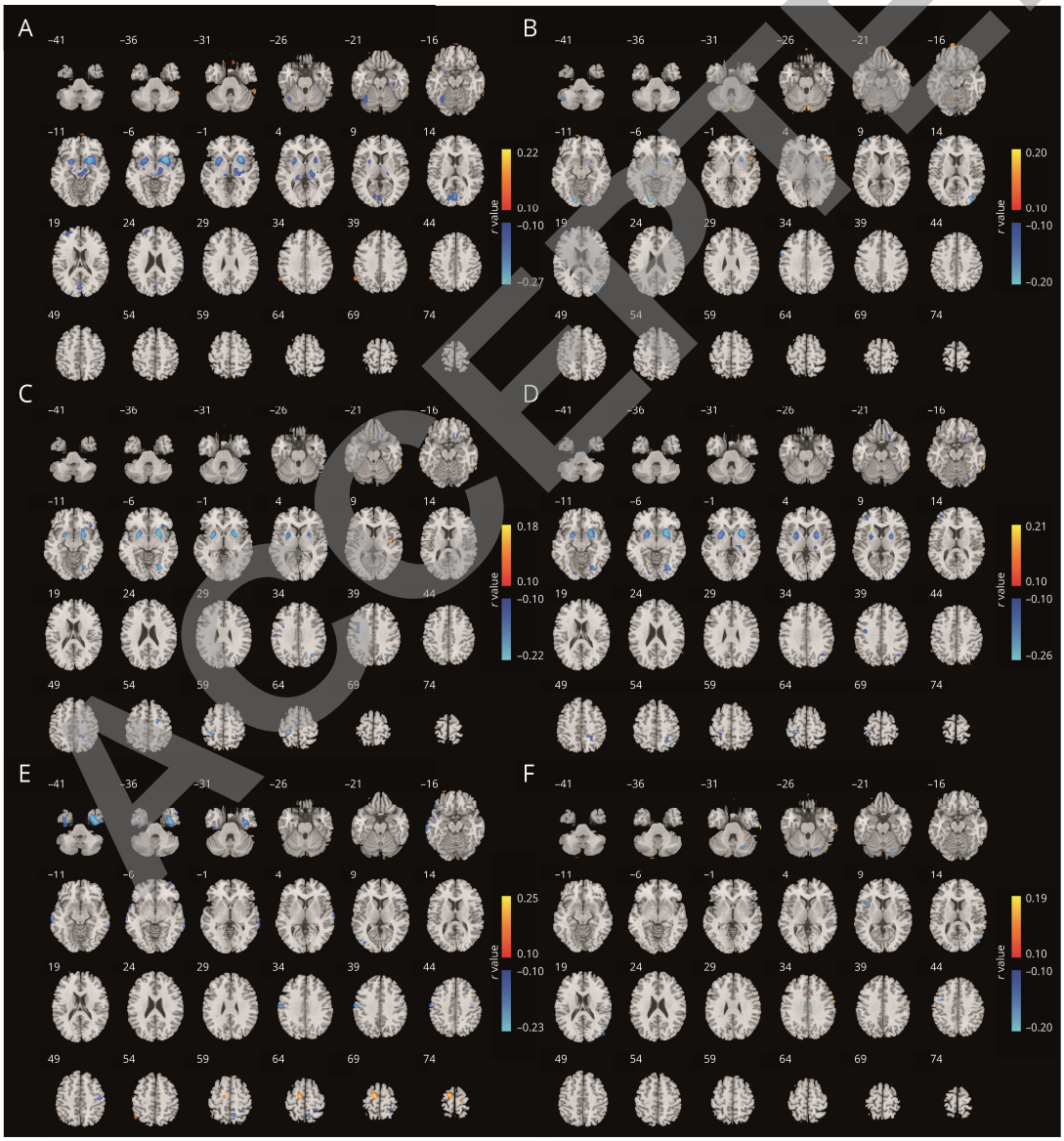

Figure 3. Dendrogram of the final hierarchical cluster solution of PD patients in the PPMI patients. The matrix under the dendrogram shows the distance of the neuroanatomical patterns between different patients. Each element (*i* row and *j* column) in the matrix indicates the difference of the neuroanatomical patterns between the *i* the participant and *j* participant.

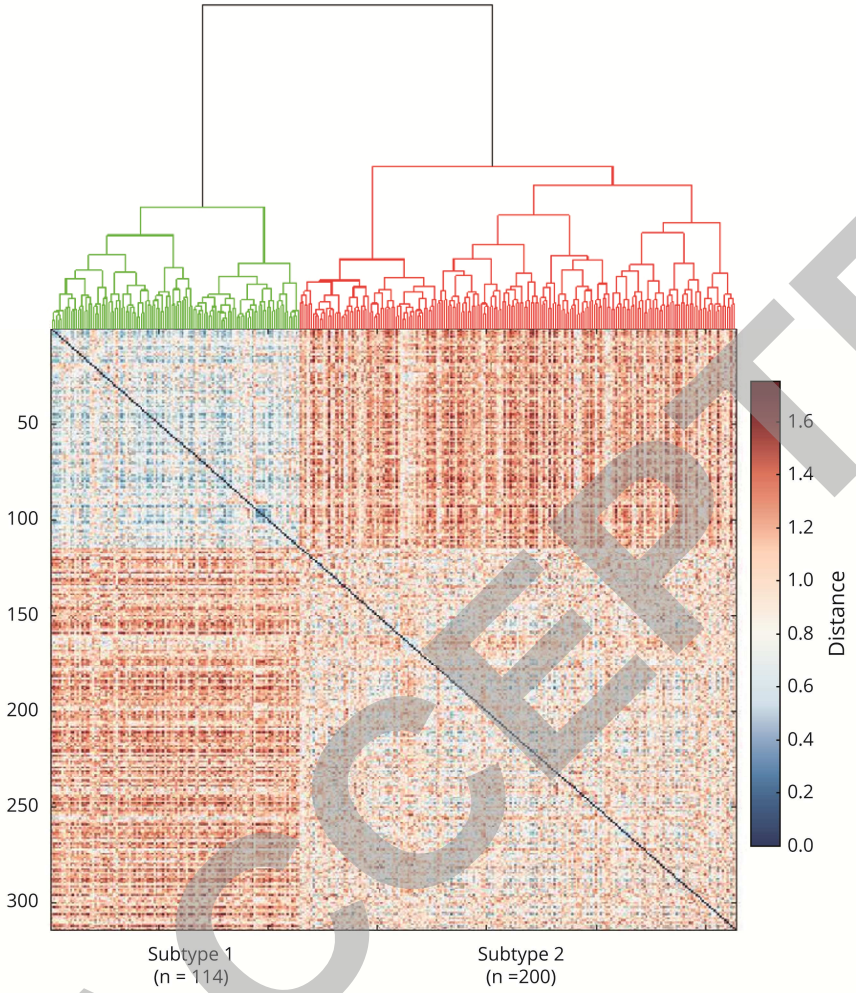

Figure 4. The different neuroanatomical patterns in the two PD biotypes compared with healthy controls. Warm color indicates higher DBM values in PD patients, and cold color indicates lower DBM values ($P < 0.005$, FDR correction). (A) The T values of comparison in DBM values between biotype 1 and controls. (B) The T values of comparison in DBM values between biotype 2 and controls.

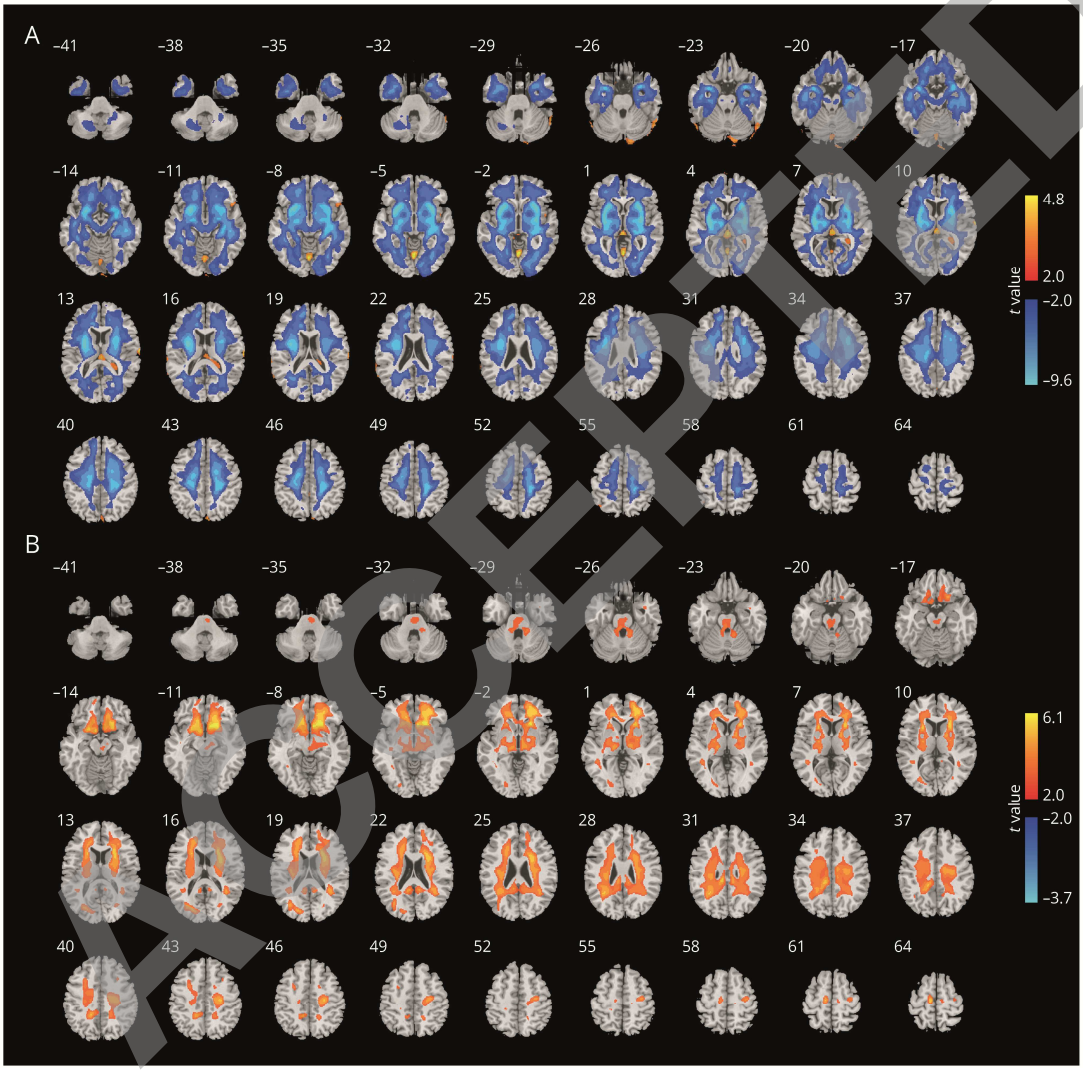

Figure 5. Longitudinal changes in outcomes of interest in different biotypes of Parkinson's disease among the PPMI patients with five years of follow-up. The asterisks indicate the statistical significance of the comparison between two biotypes in the clinical variables at the time of different follow up (* P <0.05; ** P <0.01; *** P <0.005, uncorrected for multiple comparisons). The PPMI data contains one baseline set of data and 12 follow up sets of data over five years.

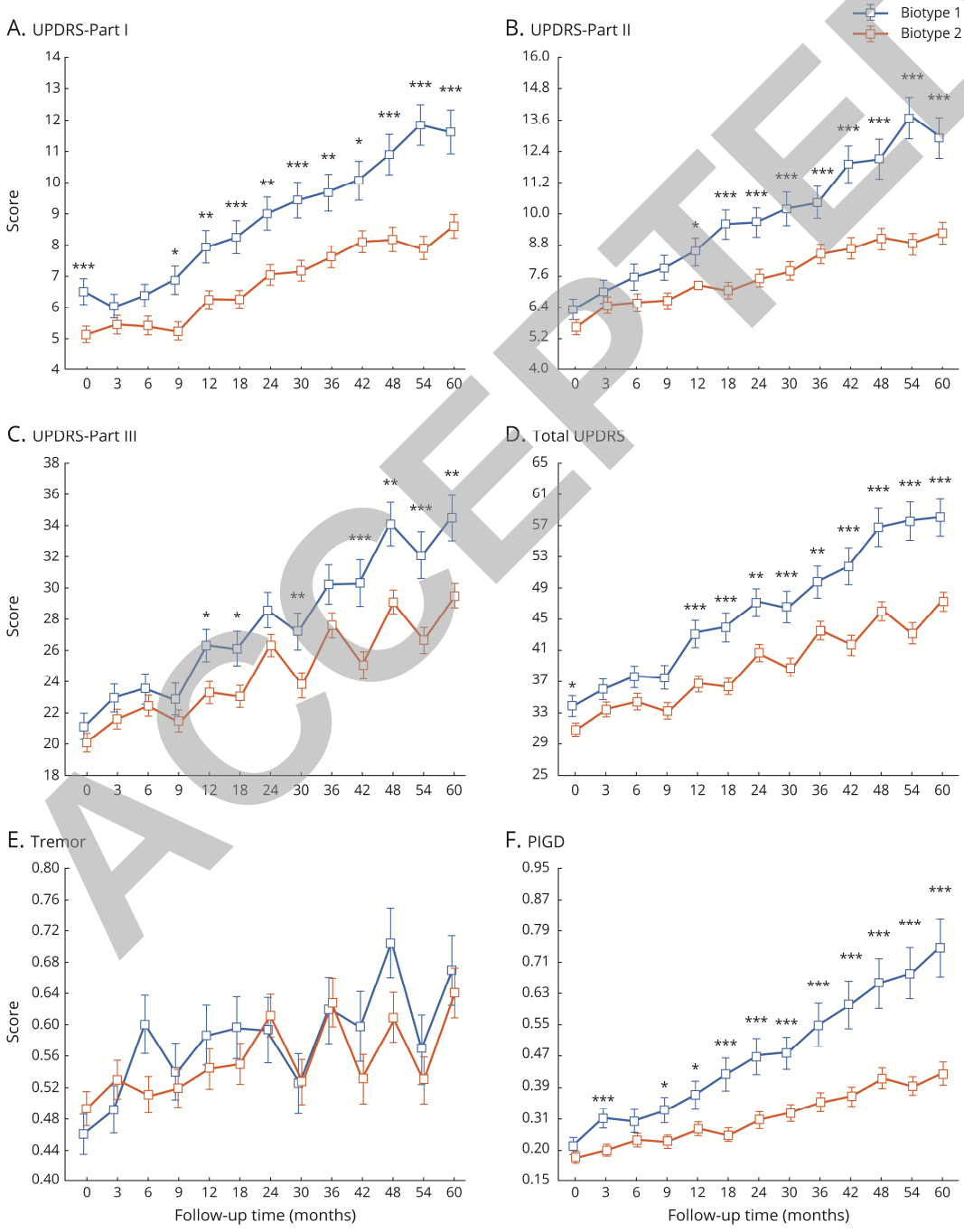

Association of specific biotypes in patients with Parkinson disease and disease progression

Linbo Wang, Wei Cheng, Edmund Rolls, et al.

Neurology published online August 14, 2020
DOI 10.1212/WNL.0000000000010498